BACHELOR THESIS

NOISE CANCELING METHODS IN POWER INVERTERS

Andrei Aursulesei

FACULTY OF ELECTRICAL ENGINEERING,
MATHEMATICS & COMPUTER SCIENCE

TELECOMMUNICATION ENGINEERING GROUP

EXAMINATION COMMITTEE
prof. dr. ir. F. Leferink
dr. ir. C. Salm
dr. ir. N. Moonen
D. Nemashkalo M.Sc.

November 2019

UNIVERSITY OF TWENTE.

Noise Canceling Methods in Power Inverters

Andrei Aursulesei, University of Twente, Enschede, Netherlands

Abstract— The power converters controlled by Pulse Width Modulation (PWM) signals exhibit harmonic noise, due to the sharp discontinuities in the PWM waveform. The objective is to develop an active filter which injects destructive interference back into the converter. In this paper, two mitigation methods named fundamental and harmonics were developed using the Fourier series analysis applied to the harmonic components of the output spectrum. The interference provided by the first method suppresses the entire output spectrum but without the fundamental component, while the interference designed with the second method suppresses only specific selected harmonic components. Both methods were applied to an ideal power inverter designed in Simulink. The methods' performances are evaluated using the Signal to Noise Ratio (SNR) values recorded on the filtered output signals and the computation times required to construct the interference signals. Based on the recorded results, the harmonics method is the most suitable to be used in the development of a more complex filter that can work in a real setup.

I. INTRODUCTION

The biggest unwanted side effect of switching power converters is that they generate harmonic noise, which can be considered as an Electromagnetic Interference (EMI) source by neighboring systems around the power converter device. These harmonics are inherited from the PWM signals that control the switches in the converter. The PWM signal is characterized by a periodic pulse waveform that switches between a maximum and a minimum level with high frequency. Since this PWM signal is real-valued and periodic, it can be modeled mathematically by a Fourier series sum. The undesired harmonics are mathematically represented by all the sinusoidal terms in the Fourier series without the first one which represents the fundamental component [1].

Because these harmonics represent an EMI source for other systems and can cause the converter itself to not function properly, various mitigation methods have been created. According to [2] the existing mitigation techniques are divided in two main categories: the ones that act at the noise source and the ones that act along the propagation path. One method of suppression at the noise source is called interleaving [3] and consists in using a modular system with identical converters connected in series or parallel. The PWM signals that control the converters are built using the same carrier and reference frequencies, but the carrier signals are shifted from each other usually by an equal fraction of the carrier cycle. Combining the output signals of each converter leads to harmonic cancelation in the modular system's output. In the propagation path, the harmonics are eliminated using passive and active filters. The passive lowpass filters suppress the frequency components that are situated after the filter's cut-off frequency. The active filters are divided in two categories: feedforward and feedback. Both are placed between the noise source and the load. The difference between them is that the feedforward filter injects a predicted destructive interference at the load, where the feedback filter measures the noise at the load and injects the anti-noise signal at the source.

One of the latest researched mitigation technique that belongs in the active filters category is called Adapted Harmonics Cancellation (AHC) [4]-[6] and was implemented on a DC-DC converter. This canceling method consists of injecting synthesized destructive interference that cancels the unwanted harmonics. The destructive interference is built using Fourier analysis of the converter's output signal. It states that each unwanted harmonic can be reconstructed in the time domain by a sinusoidal function due to its frequency domain representation. In order to construct the best time domain representations, this mitigation method uses in the feedback loop a Least Mean Square (LMS) algorithm that optimizes the parameters of the sinusoidal function in order to suppress as much as possible the specific harmonics.

Based on the latest researched suppression methods, it was decided to investigate how efficient is the AHC method applied to a power inverter. The reason for this is that the power inverter is controlled by a Sinusoidal Pulse Width Modulation (sPWM) signal, which has a more complex frequency spectrum than the PWM signal. By achieving a satisfactory suppression rate using an active filter, it can help to omit the usage of a low pass passive filter at the connection between the inverter with a load or to minimize its physical size, since its cutoff frequency can be increased. As the initial goal belongs to a complex filtering system, where its development was too difficult to be achieved in a period of time less than ten weeks, it was decided to start by investigating the suppression effect of two simpler filters compared with the AHC one. Both filters are active and use a feedback topology. The first one injects a destructive interference that suppresses the entire sPWM spectrum, but without the reference frequency. The second one injects a sum of destructive interferences that targets only those frequency components that have a magnitude higher than a certain threshold. The reasons behind choosing these two filters are that the first one offers an idealistic result that can be used as a reference for future prototype filters that will function on the real setup and the second filter is a rudimentary approach of the AHC method, the interferences are synthesized but they are not continuously adapted to achieve a certain suppression efficiency. A half-bridge topology was chosen for the inverter used in this investigation because it requires only two control signals. The investigation was done by applying the filters to the inverter's output in a simulation environment, where the suppression rates and computational times of each mitigation technique represent the evaluation parameters.

The following section is dedicated to the power inverter used in this project, where its working principle and the noise source are presented. The theory part of this paper is ended by Section III, in which the investigated canceling methods are described. In Section IV, the implementation process of these methods and the simulation setup is discussed, then in Section V, the results are presented. The paper is ending with an evaluation and conclusion section followed by a future work discussion.

II. INVERTER

Inverters are devices that convert the power produced by a DC source to a load that requires AC power. They generate an output signal with different waveform based on the circuit topology used. The most general outputs are square wave and modified sine wave. The harmonic distortion appears due to the switches that chop the voltage supply to produce the specific output waveform. The inverters are usually built from half-bridges or full-bridges connected in series or parallel depending on the output waveform's requirements. The switching gates are controlled by sPWM signals. In the following subsections, the working principle of the sPWM generator and half-bridge module used in this project are presented, followed by a mathematical model of the inverter's output signal.

A. sPWM Generator

It has been chosen to use a unipolar constant pulse frequency sPWM waveform as the control signals for the inverter's gates. The sPWM signal was created by comparing a bipolar reference signal with a bipolar carrier signal. The reference signal described by Eq. 1 is the desired signal at the output of the inverter, so in this case, it is defined by a sine function. The carrier signal is defined by a triangular wave.

$$x_{ref}(t) = A_{ref}\sin\left(2\pi f_{ref}t + \theta_{ref}\right) \tag{1}$$

In order to avoid overmodulation, the reference's amplitude is scaled by a modulation index that ensures the modulation wave is smaller than the carrier's amplitude. When the scaled reference is greater than the carrier, the comparator's output is 1 and for the other case, the output is 0 [3]. In Fig. 1 a diagram of the sPWM generator can be seen and in Fig. 2 the comparator mechanism.

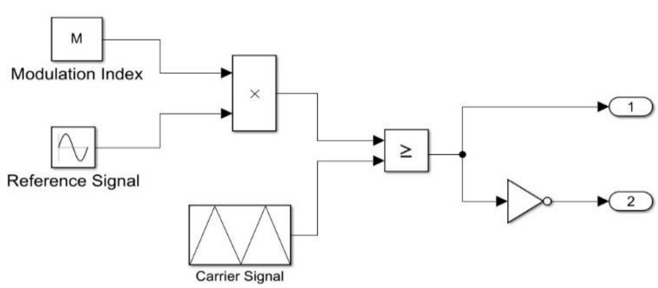

Fig. 1: 2 level sPWM generator

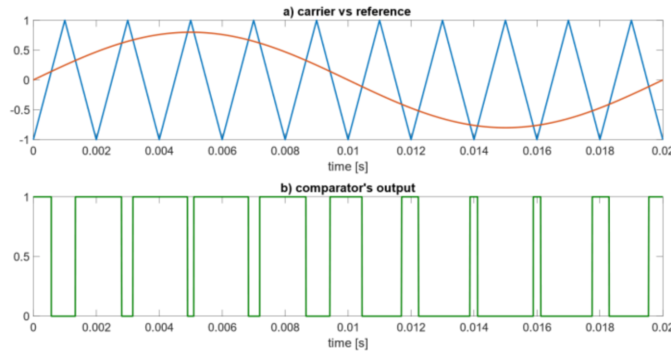

Fig. 2: sPWM development a) comparison between the reference and the carrier b) comparator's output

B. Half-bridge Module

Fig. 3 shows the inverter simulation model used in this project, which consists of a half-bridge module connected to the sPWM generator and a resistive load. The inverter works by switching on alternatively the two gates in order for the output load to have a positive voltage drop across it when the gate 1 is switched on and gate 2 is switched off, and a negative voltage drop across it when gate 1 is off and gate 2 is on. Therefore, the two control signals must be opposite to each other.

In this configuration, the output signal is defined by an sPWM waveform with $V_{max} = V_{DC}$ and $V_{min} = -V_{DC}$ and a pulse frequency equal to the carrier frequency. The output spectrum consists of a fundamental frequency component that must be equal with the reference's frequency, and unwanted harmonics, which are resulting from the switches that cut the supplied DC voltages and provide fast transitions between the maximum and minimum voltage levels. Fig. 4 and 5 show the output signal in the time domain and respectively the frequency domain.

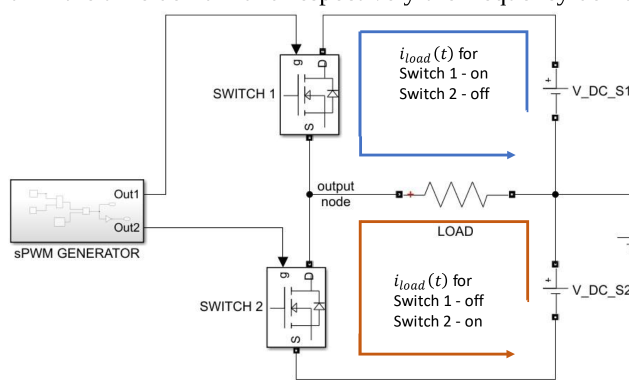

Fig. 3: Diagram of the inverter

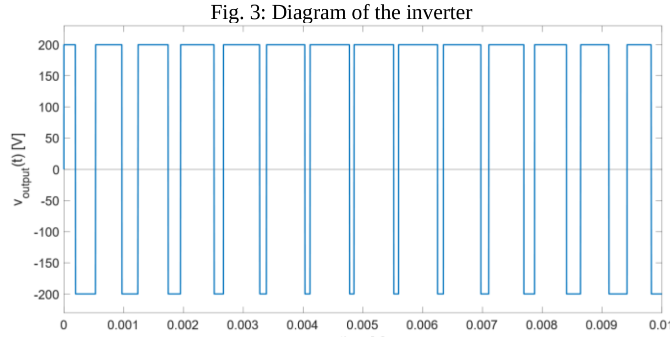

Fig. 4: Time plot of the output signal

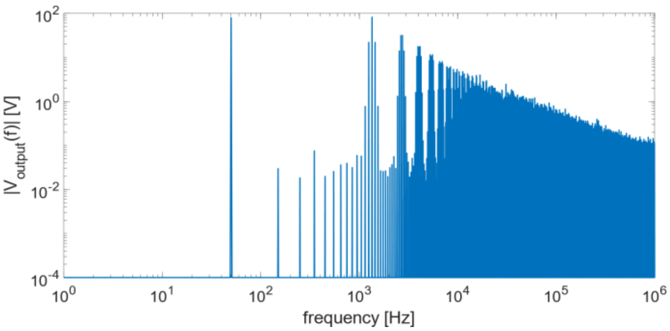

Fig. 5: Frequency spectrum of the output signal

C. Mathematical Model

For the type of modulation and the topology of the inverter used in this project, the following mathematical model is used, which is derived in [1]. It shows the specific harmonic components contained by the output signal measured over the load.

$$v_{output}(t) = V_{DC} M \cos\left(\omega_{ref} t + \theta_{ref}\right) + \quad (2)$$
$$V_{DC} \sum_{m=1}^{\infty} \frac{4}{m\pi} J_0\left(\frac{m\pi M}{2}\right) \sin\left(\frac{m\pi}{2}\right) \cos[m(\omega_c t + \theta_c)] +$$
$$V_{DC} \sum_{m=1}^{\infty} \sum_{\substack{n=-\infty,\\ n\neq 0}}^{\infty} \frac{4}{m\pi} J_n\left(\frac{m\pi M}{2}\right) \sin\left[\frac{(m+n)\pi}{2}\right] \cdot$$
$$\cos\left[m(\omega_c t + \theta_c) + n\left(\omega_{ref} t + \theta_{ref}\right)\right], m \in \mathbb{N}^*, n \in \mathbb{Z}^*,$$

where M represents the modulation index, J_n denotes the Bessel function of the first kind for nth order, ω_{ref} and ω_c the reference and carrier angular frequencies and θ_{ref} and θ_c the reference and carrier phases. The first element in the Eq. 2 represents the reference signal with its amplitude scaled by the product between the DC voltage and modulation index. The second term in the sum represents the carrier frequency and its harmonics, which are denoted by the $m\omega_c$. The last term in the sum represents the sideband harmonics at the carrier harmonics, which are denoted by $m\omega_c + n\omega_{ref}$. Fig. 6 shows an approximated spectrum described by Eq. 2.

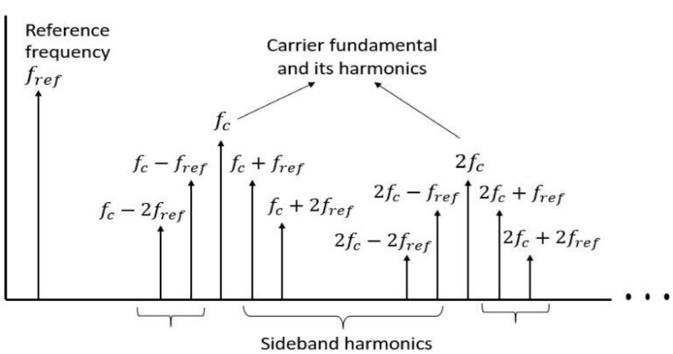

Fig. 6: Approximated frequency spectrum of the inverter's output

III. CANCELING METHODS

The two filters used in this project are implementing the following active canceling methods discussed in this section: Fundamental and Harmonics. Both methods focus on providing a destructive interference signal that will affect the output signal by suppressing its harmonics as much as possible. The fundamental method produces a destructive interference designed to suppress the entire output spectrum without the reference frequency, while the harmonics method delivers destructive interferences designed for specific harmonic components in the output spectrum.

The feedback configuration was chosen as the main final goal is to create a type of continuously adaptive filter that can change the synthesized interference according to the disturbances to which the system might be subjected.

Both mitigation methods are based on the Fourier series analysis [7] applied on the inverter's output signal. Which states that any periodic real-valued signal $x(t)$ with period T can be expressed as

$$x(t) = c_0 + \sum_{h=1}^{\infty} 2|c_h| \cos\left(\frac{2h\pi t}{T} + \measuredangle c_h\right), h \in \mathbb{N}^* \quad (3)$$

where c_h represents the Fourier coefficient

$$c_h = \frac{1}{T}\int_0^T x(t) \exp\left(-j\frac{2h\pi t}{T}\right) dt, h \in \mathbb{N}^*. \quad (4)$$

As a consequence of Fourier analysis, the development of the interference signal from both methods can be done via two approaches: in time domain or in frequency domain.

In the next subsections, the working principles of each mitigation method are going to be presented for an ideal setup, where the following effects:

- signal delays,
- dead time insertion,
- internal or external noise sources,
- passive suppression

caused by the limitations of a real setup, are not considered, in order to simplify the understanding of the basic mechanisms in the harmonics active filtering development.

A. Method: Fundamental

The goal of this method is to provide an interference signal that must suppress the entire frequency spectrum of the output signal, but without the fundamental component, which is equal to the frequency of the reference signal used in the sPWM generator. The theoretical outcome of this method applied to an ideal scenario can be used as a reference for the development of more complex active filters that can deliver good suppression rates of the harmonic components on a real setup.

1) Time domain approach

In the time domain approach, the interference signal is developed using the information about the reference frequency used in the sPWM generator and characteristics of the fundamental frequency of the signal at the inverter's output. The top-level diagram of this approach can be seen in Fig. 7.

The active filter first acquires the output signal $y_{acquired}(t)$, which includes the entire frequency spectrum. Next, it constructs the reference signal $y_{fund}(t)$ that must contain only the reference frequency. Afterward, the interference is created by inverting the difference between the acquired signal and the reconstructed reference signal. Finally, the interference is injected at the output of the inverter and is defined mathematically by the following equation:

$$y_{injected}(t) = -\left(y_{acquired}(t) - y_{fund}(t)\right). \quad (5)$$

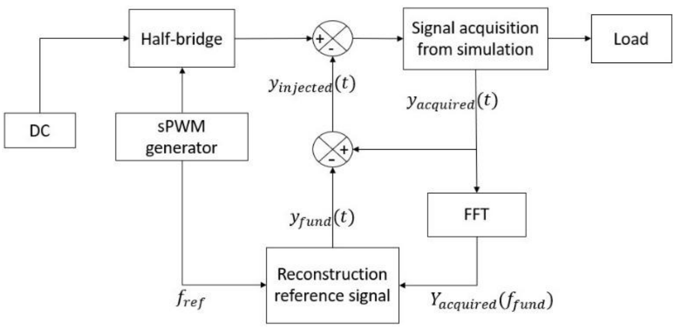

Fig. 7: Top-level diagram of the cancelation system based on the fundamental method with time domain approach

The reconstruction block of the reference signal uses Eq. 3 and it needs the following information:

- reference frequency f_{ref},
- fundamental component's magnitude A_{fund},
- fundamental component's phase θ_{fund}.

The reference frequency is taken from the sPWM generator block, while the amplitude and the phase shift of the fundamental signal are taken from the inverter's output. The last two variables can be determined from the Fourier transform of the output signal. The amplitude (Eq. 6) and the phase (Eq. 7) are determined from applying the magnitude and the argument operations on the complex number $Y_{acquired}(f_{fund})$ that represents the fundamental frequency of the output signal in the Fourier domain. The complex number $Y_{acquired}(f_{fund})$ is selected from the output spectrum by searching the frequency component that is equal to the reference frequency f_{ref}.

$$A_{fund} = 2\left|Y_{acquired}(f_{fund})\right| \quad (6)$$

$$\theta_{fund} = \measuredangle Y_{acquired}(f_{fund}) \quad (7)$$

The reconstructed reference signal (Eq. 8) is then calculated using Eq. 3, where c_h is substituted with $Y_{acquired}(f_{fund})$ and c_0 is discarded since the reference signal (Eq. 1) does not contain a DC offset.

$$y_{fund}(t) = A_{fund}\cos(2\pi f_{fund}t + \theta_{fund}). \quad (8)$$

2) Frequency domain approach

In the frequency domain approach, the destructive interference signal is developed taking the reference frequency from the sPWM generator and the Fourier transform applied on the acquired signal. The top-level diagram of this approach can be seen in Fig. 8. The fundamental frequency elimination block constructs the destructive interference signal in the frequency domain by eliminating the frequency components from the acquired signal's spectrum that are equal with the positive and negative fundamental frequency. The cancelation system finds the complex values that represent the above-mentioned frequency components in the Fourier transform of the acquired signal by searching the frequency components that are equal to the positive and negative reference frequency f_{ref}. Afterward, the selected complex values are equalized to zero. The resulted interference spectrum is transformed to the time domain by means of the IFFT and inverted to create the destructive aspect, and then the outcome is injected back into the system. The injected signal is defined in the frequency domain by the following equation:

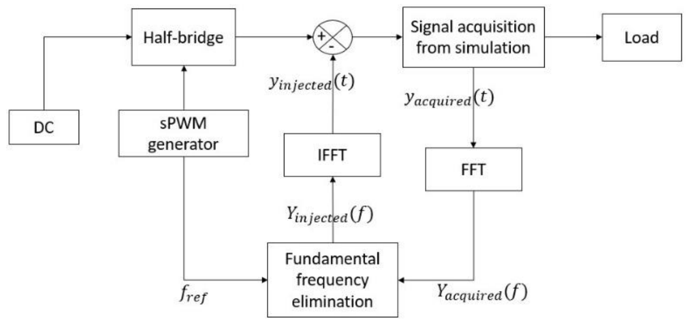

Fig. 8: Top-level diagram of the cancelation system based on the fundamental method with frequency domain approach

$$Y_{injected}(f) = \begin{cases} Y_{acquired}(f), & f \neq \pm f_{fund} \\ 0, & f = \pm f_{fund} \end{cases}. \quad (9)$$

The reason why also the negative fundamental component is set to zero is that the signal must preserve its symmetry in order for the result of the inverse Fourier transform to be a real-valued waveform as the acquired signal from where the entire process started. Therefore, the injected signal is obtained in the time domain by the following equation:

$$y_{injected}(t) = \mathcal{F}^{-1}\{Y_{injected}(f)\} \quad (10)$$

Fig. 9 shows the magnitude spectrum of the injected signal where only the peak corresponding to the fundamental frequency is discarded. In Fig. 10 a comparison is made in the frequency domain between the simulated output, $y_{acquired}(t)$ and the theoretical desired output, which is defined by:

$$y_{outcome}(t) = y_{acquired}(t) + y_{injected}(t). \quad (11)$$

In Fig. 11 the following signals used by the fundamental method are depicted in the time domain:

- The acquired signal, the sPWM waveform,
- The destructive interference signal, the curved sPWM waveform,
- The desired theoretical inverter output, the amplified reference signal.

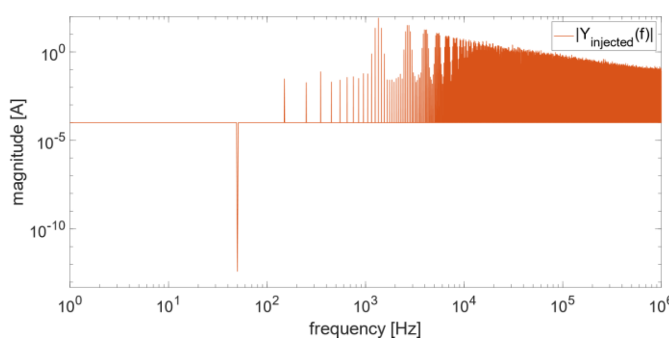

Fig. 9: Magnitude spectrum of the destructive interference signal

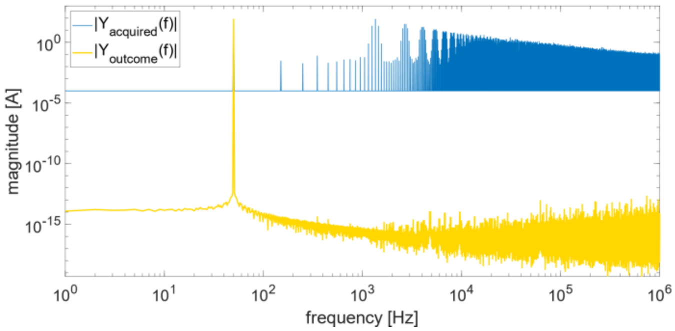

Fig. 10: Magnitude spectrum comparison between the desired theoretical output signal and the acquired signal

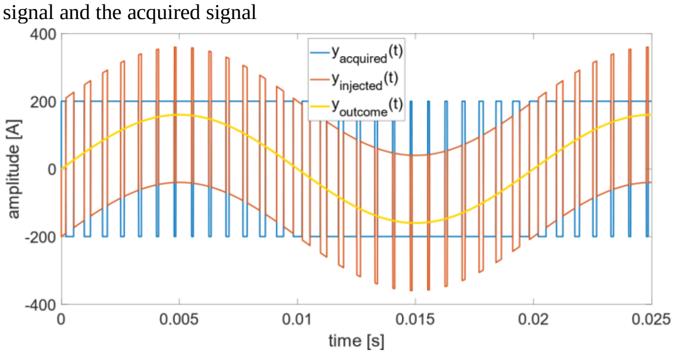

Fig.11: Time plot of the signals used in the fundamental method and the desired theoretical output

B. Method: Harmonics

This mitigation method is based on the harmonic distortion principle, where the harmonic components that have a large amplitude represent the main cause for the distortion that affects the fundamental signal present at the inverter's output port. The mitigation system provides a destructive interference signal which should suppress only those harmonics that have a magnitude larger than a certain limit. In this way, the system can omit the processing of harmonic components that do not contribute significantly to the distortion of the desired output signal.

1) Time domain approach

In this approach, the cancelation system creates the interference signal by constructing time domain replicas of the targeted harmonics using information taken from the representation of the acquired signal in the Fourier domain. The top-level diagram of this approach can be seen in Fig. 12. The selection of the harmonics is done by the Magnitude threshold block, which compares the magnitude of each frequency with a threshold. If a frequency component $Y_{acquired}(f_n)$ passes the test, its frequency f_n, magnitude (Eq. 12) and phase (Eq. 13) information are used by the Harmonics modeling block to construct a time domain model (Eq. 14) of that specific harmonic $y_n(t)$. This approach assumes that each harmonic component can be represented in time domain by the Fourier series formula defined in Eq. 3, where c_h is substituted with the harmonic components of $Y_{acquired}(f)$ that are above the threshold and c_0 is set to zero since the harmonic signals do not contain a DC offset.

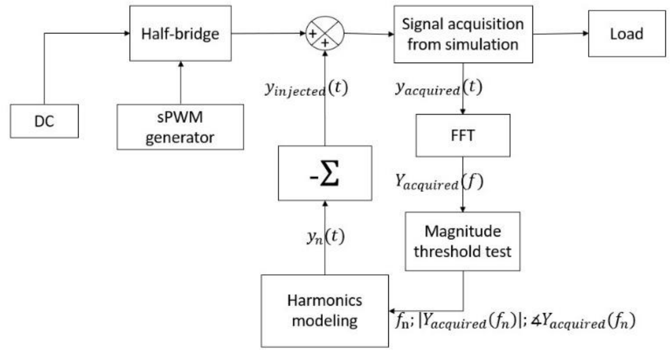

Fig. 12: Top-level diagram of the cancelation system based on the harmonics method with time domain approach

$$A_n = 2|Y_{acquired}(f_n)| \tag{12}$$
$$\theta_n = \measuredangle Y_{acquired}(f_n) \tag{13}$$
$$y_n(t) = A_n \sin(2\pi f_n t + \theta_n)\,, \tag{14}$$

where n represents the index for each harmonic component that passed the threshold test. The destructive interference signal is defined by summing all the time domain harmonic representations and then multiply the sum with -1 as shown in Eq. 15.

$$y_{injected}(t) = -\sum_{n=1}^{\infty} y_n(t) \tag{15}$$

2) Frequency domain approach

The frequency domain approach calculates the time replicas that form the interference signal, using the inverse Fourier transform. The top-level diagram can be seen in Fig. 13.

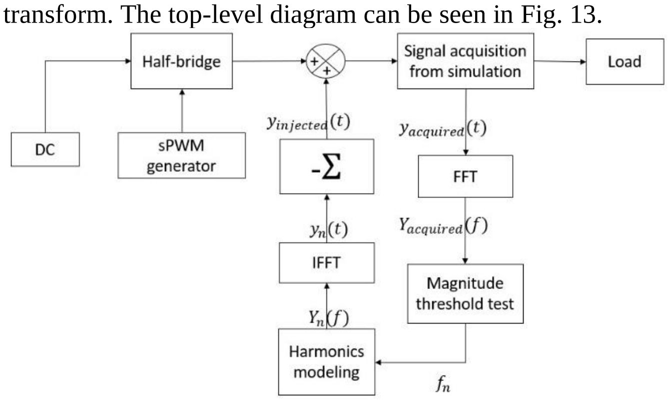

Fig. 13: Top-level diagram of the cancelation system based on the harmonics method with frequency domain approach

The algorithm creates a new signal in the frequency domain for each frequency component of the acquired signal from the simulation that has a magnitude above the threshold. The new spectrum (Eq. 16) contains only the specific frequency and its negative counterpart. The time domain model of each harmonic (Eq. 17) is reconstructed by the result of the inverse Fourier transform applied on the newly constructed spectrum $Y_n(f)$.

$$Y_n(f) = \begin{cases} Y_{acquired}(f), & f = \pm f_n \\ 0, & f \neq \pm f_n \end{cases} \tag{16}$$
$$y_n(t) = \mathcal{F}^{-1}\{Y_n(f)\}, \tag{17}$$

where n and represents the index for each harmonic component that passed the threshold test. Then the injected signal is calculated in the same manner as in the time domain approach (Eq.

15). In Fig. 14 it can be seen the magnitude spectrum of the injected signal which is composed only of the frequency components that passed the threshold test which belongs to the carrier harmonics and the sideband harmonics.

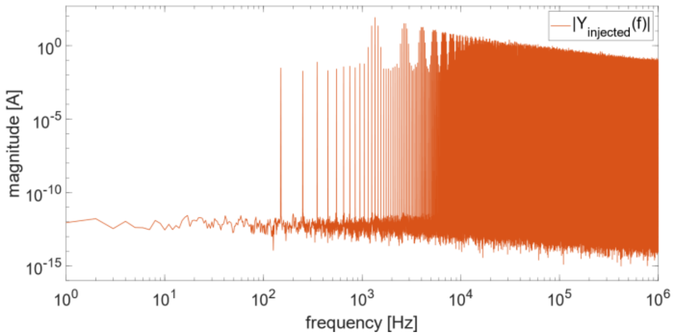

Fig. 14: Magnitude spectrum of the destructive interference signal

In Fig. 15 the comparison between the theoretical desired output signal, defined in Eq. 11, and the acquired signal is shown in the frequency domain, where the desired spectrum has only the harmonics suppressed.

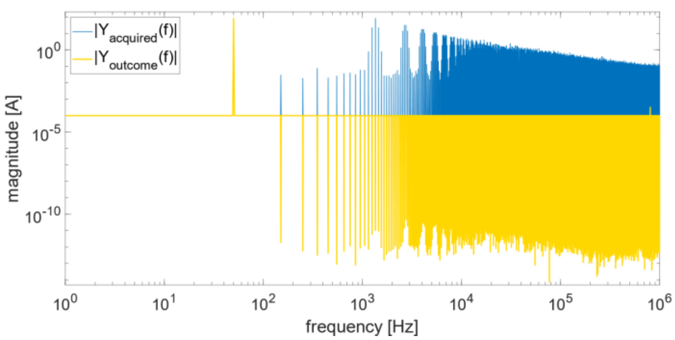

Fig. 15: Magnitude spectrum comparison between the desired output signal and acquired signal

In Fig. 16 the following signals used by the harmonics method are depicted in the time domain:

- The acquired signal, the sPWM waveform,
- The destructive interference signal, the curved sPWM waveform,
- The desired theoretical inverter output, the amplified reference signal.

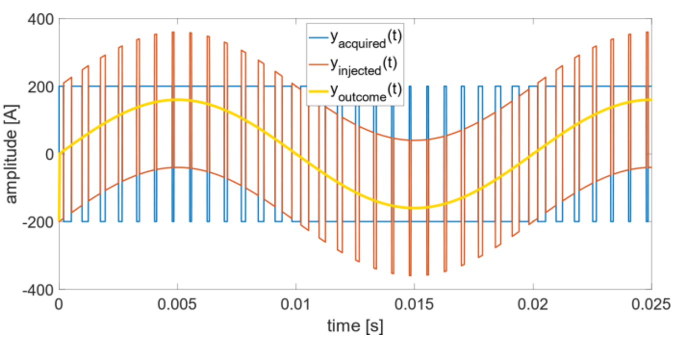

Fig. 16: Time plot of the signals used in the harmonics method and the desired theoretical output

By comparing the theoretical desired output signals derived using both mitigation methods for the ideal case, from Fig. 10, 11, 15 and 16, it is expected that both methods will provide similar suppression rates while they are applied to a simulation setup which includes non-ideal injection circuitry described in the following section. Based on the computing complexity of the mitigation algorithms shown in Figs. 7, 8, 12 and 13, it is estimated that for each canceling method, the time approach will need less computation time than the frequency approach. Moreover, it is expected that the harmonics method will require more computational time than the fundamental methods since it has to construct interferences for each harmonic that passes the threshold test, while the fundamental method provides only one interference signal.

IV. SIMULATION SETUP

The theory presented in the previous section describes the working principle of the proposed filters in an ideal scenario. In this section, a simulation setup is described that introduces an injection circuit and also add extra disturbances in order to test the filters' capabilities and understand what has to be configured in their design in order to achieve satisfactory performance when applied in a real setup.

A. Inverter Setup

The suppression methods described in the previous section were simulated using the circuit shown in Fig. 17, and where the blocks of sPWM generator and half-bridge consists of the diagrams presented in Fig. 1 and 3. The DC voltage sources provide 200 V and respectively -200 V to the half-bridge switches. The reference signal (Eq. 1) and the carrier signal used in the sPWM generator were built by choosing the following variables:

- reference frequency $f_{ref} = 50$ Hz;
- reference phase $\theta_{ref} = 0$ rad;
- reference amplitude $A_{ref} = 1$;
- modulation index $M = 0.8$;
- carrier frequency $f_c = 1350$ Hz;
- carrier phase $\theta_c = 0$ rad;
- carrier amplitude $Ac = 1$.

The reference frequency value was chosen in order to simulate the utility frequency. The higher the carrier frequency is, the less distorted the output signal will be. Since the scope is to investigate the mitigation of the harmonic noise using active filtering methods, it was chosen a low value for the carrier frequency.

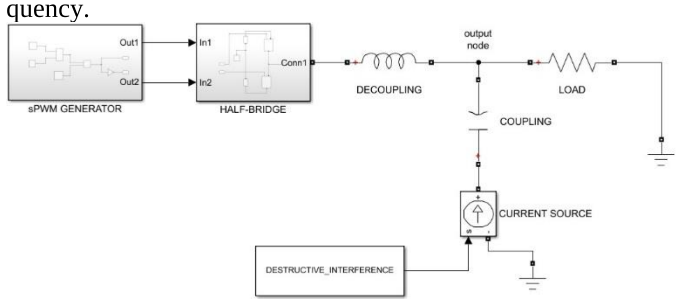

Fig. 17: Final circuit

B. Injection Setup

According to the previously chosen frequency variables and the mathematical model presented in Eq. 2, the harmonic noise has a frequency spectrum that is delimited relatively by the following interval $[150\ \mathrm{Hz}, \infty)$, where the left boundary value represents the left outermost sideband harmonic of the carrier frequency, as it can be visualized in Fig. 5. The destructive interference signal $y_{injected}$ is produced by an ideal current source. In order for the injection process to work, other two components were added to the system. Firstly, an ideal coupling capacitor which suppresses the frequencies below 150 Hz and secondly, an ideal decoupling inductor which makes sure that the destructive interference travels mainly towards the load and not into the half-bridge. The produced current is injected at the output node via the coupling capacitor as is shown in Fig. 17.

The capacitance $C_{decoupling}$ was chosen accordingly to the following formula:

$$Z_{coupling}(f) = \frac{1}{2\pi f C_{coupling}}. \tag{18}$$

Using the harmonics' spectrum, the highest impedance seen by the destructive interference signal would be for $f = 150$ Hz. For this frequency, a capacitive impedance of approximately 10 Ω was considered suitable for blocking the low frequencies and respectively the capacitance $C_{coupling}$ of 100 µF.

Setting the load impedance Z_{load} to be equal to 1 Ω and assuming the impedance of the half-bridge to be negligible, the impedance inequality that defines the traveling path of the injected interference signal is simplified to:

$$Z_{decoupling}(f) > Z_{load}(f), \forall\, f \in [150\ \mathrm{Hz}, \infty). \tag{19}$$

Since the impedance of the inductor is directly proportional to the frequency,

$$Z_{decoupling}(f) = 2\pi f L_{decoupling}, \tag{20}$$

the inductance (Eq. 21) calculated for 150 Hz, would be suitable for the entire harmonics' spectrum.

$$L_{decoupling} > \frac{1\ \Omega}{2\pi \cdot 150\ \mathrm{Hz}} \approx 1\ \mathrm{mH} \tag{21}$$

The unwanted side effect of using a passive element for decoupling is that it distorts the output signal. In this configuration, the inductor and the resistor are forming a low pass filter with a cut off frequency of approximately 150 Hz. The passive suppression is shown in Fig. 18 and 19, where a comparison between the output current simulated without and with the coupling and decoupling elements is shown both in time and frequency domain.

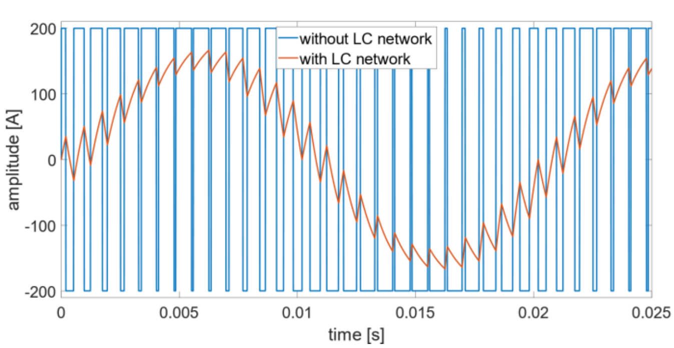

Fig. 18: The effect of passive suppression on the output current in time domain

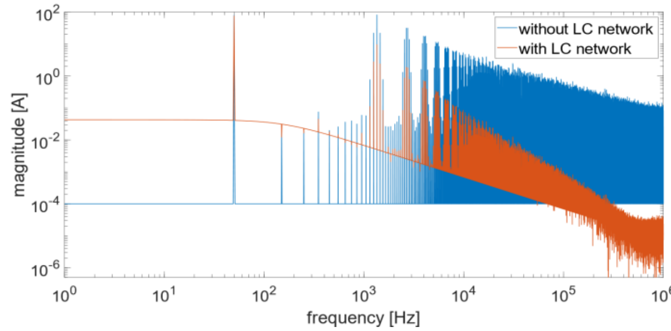

Fig. 19: The effect of passive suppression on the output current in frequency domain

C. Disturbances Setup

Since in a real environment the inverter is subjected to different types of disturbances, it was decided to investigate these effects on the filters' performance. The disturbances that might affect the inverter and the filter are:

- Thermal noise in resistive components,
- Shot noise in semiconductors
- Quantization noise in ADCs and DACs,
- EMI arose from external systems.

The disturbances investigation was done by injecting additive white noise at the inverter output port. The injected noise was characterized by a power spectral density of $0.001\ \mathrm{V^2 Hz^{-1}}$. The performance of each method with its approaches was tested using three disturbances cases:

1) No additive white noise
2) Constant additive white noise
3) Additive white noise

In the first case it was examined the filters' ability to build destructive interference signals for the passively filtered harmonic components, while in the last two cases, it was investigated the filters' performance in suppressing the white noise components in the output spectrum and the harmonic components distorted by the added white noise and by the passive filter.

D. Simulation Setup

The simulation setup was built using Simulink and Matlab. The circuit was designed in Simulink and the algorithms of each method were implemented in Matlab. The testing procedure of each suppression method with its approaches works by running sequentially the simulation two times for each disturbance case. During the first simulation run, the destructive interference block is set to 0 and the current at the load is measured. This data is exported to Matlab where it acts as input for the algorithm that will generate the destructive interference signal. When the algorithm finishes to construct the interference signal, the second simulation run begins. This time the destructive interference block contains the noise canceling signal that is injected into the output node and then the result is measured again over the load.

The distinction between the last two disturbance cases is that in the constant additive white noise case, it is used the same additive white noise for both simulation runs. While in the third case, the second simulation run contains a different additive white noise, for the scope of approaching the influences of a real white noise source.

The investigation was evaluated by the following parameters: the SNR observed at the inverter output and the computation time required by each algorithm to construct the destructive interference. The SNR used here is defined by the power ratio between the fundamental signal and the rest of the frequency components in the output spectrum.

V. RESULTS

In this section, the computation times for building the interference and the pre-filtering and post-filtering SNR values are going to be presented for each suppression method.

A. Method: Fundamental

The measured computation times of the fundamental method algorithms are shown in Table I. In each disturbance case, the algorithm implementing the time domain approach was approximately two times faster than the algorithm of the frequency domain approach.

TABLE I: Running times of the fundamental method's algorithms

Disturbance Case	1	2	3
	Time [s]		
Time approach	0.049	0.048	0.047
Frequency approach	0.105	0.106	0.105

The SNR results are shown in Table II. Both approaches are providing the same attenuation performance for each disturbance case. By comparing with the pre-filtering SNR values, the fundamental method improved the output SNR with 18.9 dB in the first disturbance case and with 28.3 dB in the second case. However, in the last case, the observed SNR was worsened by 2.6 dB. In Figs. 20, 21, 22 and 23 the output signal is shown in time and frequency domain, before and after injecting the destructive interference derived with the fundamental method for the first two disturbance cases. Fig. 24 shows the attenuation performance recorded on the output signal during the third disturbance case, where it can be observed that only the harmonic components were attenuated.

TABLE II: SNR measured before and after the injection of the fundamental method's algorithms

Disturbance Case	1	2	3
	SNR [dB]		
Before injection	17.0	7.2	7.2
Time approach	35.9	35.5	4.6
Frequency approach	35.9	35.5	4.6

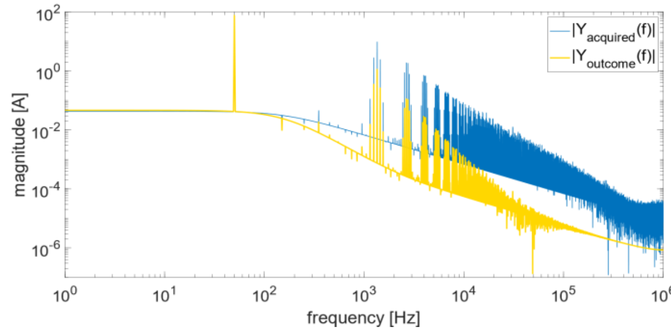

Fig. 20: Output spectrum before and after filtering with fundamental method in the case without additive white noise

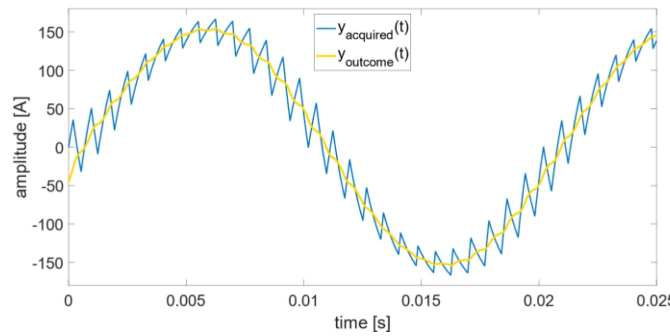

Fig. 21: Output signal before and after filtering with fundamental method in the case without additive white noise

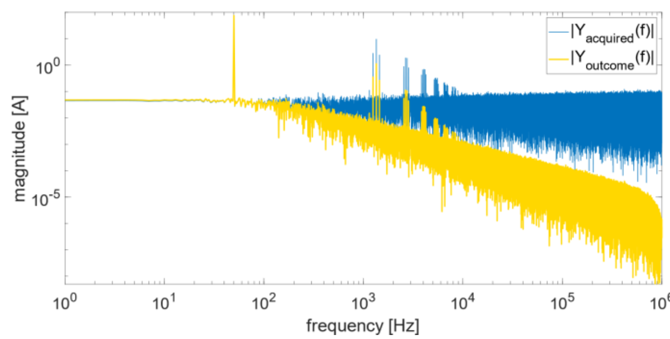

Fig. 22: Output spectrum before and after filtering with fundamental method in the case with constant additive white noise

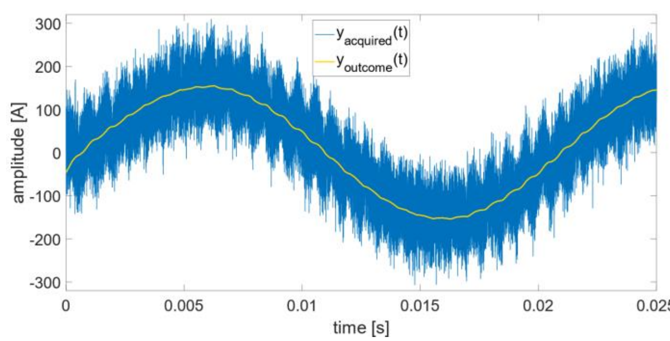

Fig. 23: Output signal before and after filtering with fundamental method in the case with constant additive white noise

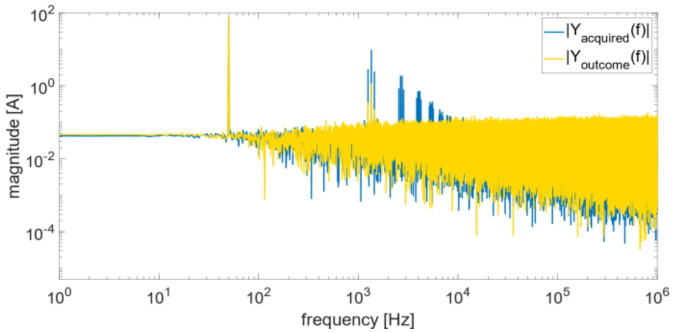

Fig. 24: Output spectrum before and after filtering with fundamental method in the case with variable additive white noise

B. Method: Harmonics

Compared with the previous mitigation method, the SNR values and computation times of the harmonics method are dependent on the threshold value. This happens because the threshold value sets the number of the frequency components in the output spectrum that are going to be processed, as shown in Table III.

TABLE III: Threshold value in relation with the number of processed frequency components

Disturbance Case	1		2	
Threshold [A]	0.05	0.07	0.05	0.07
Number of processed frequency components	52	41	75443	7492

Table IV shows the registered computation times of the harmonics method algorithms, with the threshold was set to 0.07 A. The time approach was faster than the frequency approach in each disturbance case.

TABLE IV: Running times for harmonics method's algorithms

Disturbance Case	1	2	3
	Time [s]		
Time approach	1.33	468.23	461.19
Frequency approach	3.93	680.15	681.97

The SNR results provided by the algorithms of the harmonics method with the threshold was set to 0.07 A, are shown in Table V. Both approaches are providing the same attenuation performance for each disturbance case.

TABLE V: SNR measured before and after the injection of the harmonics method's algorithms

Disturbance Case	1	2	3
	SNR [dB]		
Before injection	17.0	7.2	7.2
Time approach	35.6	7.9	7.5
Frequency approach	35.6	7.9	7.5

In the first disturbance case, the SNR was improved with 18.6 dB from the value recorded before the injection. However, the SNR recorded a very small improvement in the cases with additive noise; 0.7 dB in the second case and 0.3 dB in the third case. In Fig. 25 and 26 the output signal is shown in time and frequency domain, before and after injecting the destructive interference derived with the harmonics method for the case with no added disturbance.

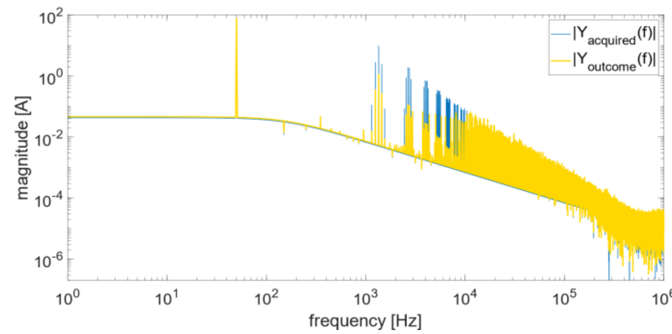

Fig. 25: Output spectrum before and after filtering with harmonics method in the case without additive white noise

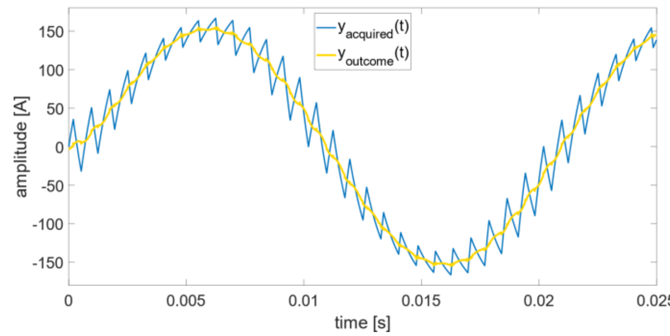

Fig. 26: Output signal before and after filtering with harmonics method in the case without additive white noise

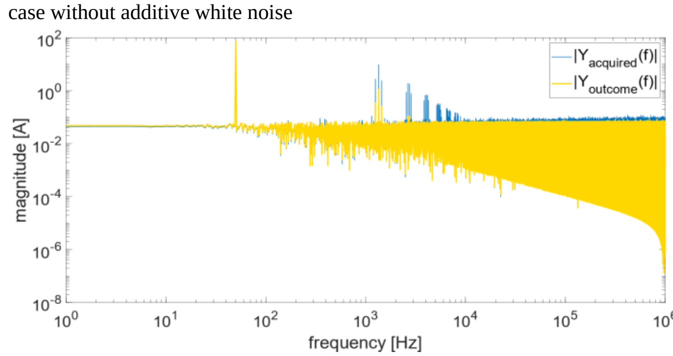

Fig. 27: Output spectrum before and after filtering with harmonics method in the case with constant additive white noise

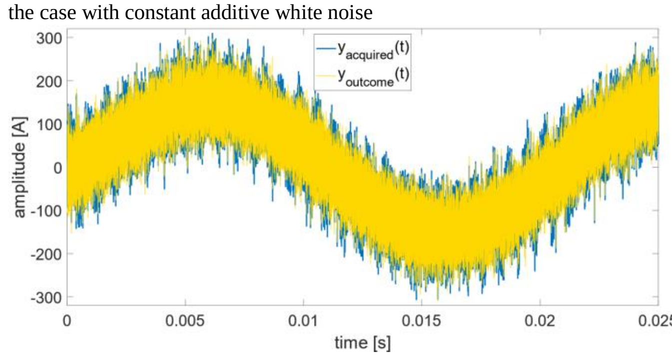

Fig. 28: Output signal before and after filtering with harmonics method in the case with constant additive white noise

In the second and the third disturbance cases, the harmonics method managed to attenuate the harmonics, where the suppression difference is presented in Figs. 27 and 29. However, the present white noise was still enough to distort the output signal as it can be seen in Fig. 28, where the influences of the constant white noise are depicted on the output signals.

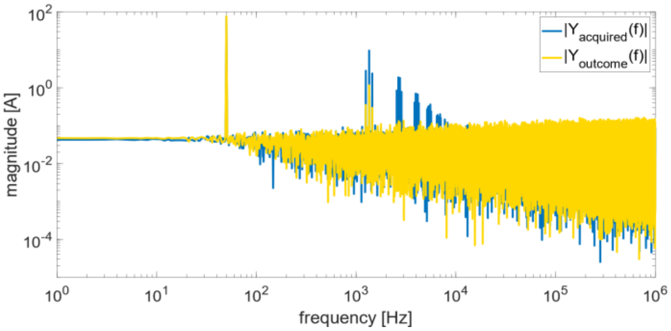

Fig. 29: Output spectrum before and after filtering with harmonics method in the case with variable additive white noise

Due to the poor attenuation performance achieved in the third disturbance case (Tables II and V), the plots that describe the relation between the pre and post filtering output signals simulated for each method were not presented. Both omitted plots are similar to Fig. 28 and therefore they do not provide more significant information.

VI. EVALUATION + CONCLUSION

This section presents the performance evaluation of the two approaches and the two attenuation methods based on the suppression rates and computation times achieved in each disturbance case.

A. Performance Evaluation of the Time and Frequency Approaches

By comparing Tables I and IV, it was established that during the simulation of each mitigation method, the time approach used for deriving the synthesized interference signals was faster than the frequency approach. This difference was expected, since the frequency approach of each method has to deal twice with the time complexity of the FFT algorithm, while the time approach uses only once the FFT algorithm. By examining Tables II and V, both the time and the frequency approaches provided the same SNR result when they were simulated for each mitigation method in each disturbance case. Which confirmed the prediction, since the information can be manipulated in both domains in order to achieve the same result. Based on the previous comparisons, the most useful approach to be used in the development of a more complex filter will be the time domain approach, mainly because it requires less computation time.

B. Performance Evaluation of the Fundamental and Harmonics Methods

Another noticeable aspect with respect to the computation time taken from Tables I and IV is that the fundamental method is faster than the harmonics method. This was expected since the fundamental technique computes only one interference signal, while the harmonics technique, based on the chosen threshold value, has to derive more than one interference signal. However, it is considered that the running times of the harmonics technique are too long, and they can be improved by finding a better Matlab implementation of the algorithm described in III-B. The biggest drawbacks of the current algorithm are the usage of a for loop to construct each interference and the built-in function called arayfun, which searches the output spectrum for the frequency components that have a magnitude higher than the threshold value.

From a harmonic noise suppression point of view, both methods can achieve the same SNR values when simulated in the ideal case, where the inverter is not affected by extra disturbances besides its inherent harmonics from the control signals as it is presented in Tables II, V, and Figs. 20, 21, 25, 26.

The fundamental method managed in the second disturbance case to suppress the constant white noise and the inherent harmonics as presented in Table II and Fig. 22. However, in the last destructive case, it turned out that the destructive interference designed to suppress the white noise acted as more noise when it was injected into the inverter's output. Even if the destructive interference managed to suppress the harmonic components as it is shown in Fig. 24. These results were expected because the synthesized destructive interference is built by inverting the acquired output signal and the Fourier series approximation was used only to discard the reference frequency component, which satisfies the conditions stated in the introduction of section III. As the fundamental method assumes that during the process of deriving the interference, the output signal is stationary, it can be concluded that the constant components in the output spectrum can be mitigated, whereas the non-stationary frequency components cannot be suppressed.

The harmonics method managed in the last two destructive cases to suppress the harmonics that were above the threshold as it is pictured in Figs 27 and 29. However, it was anticipated for this method to provide a larger attenuation for the selected harmonics in each disturbance case. According to the Eq. 2, the selected harmonics are representing in time domain sinusoidal signals, which are real-valued and periodic. Therefore, they respect the conditions for applying the Fourier series analysis described in the introduction of section III. Due to limited processing power provided by the laptop used for simulations, the threshold was set just below the maximum amplitudes of the noise floor present in the last two disturbance cases, in order to decrease the number of processed frequency components. Therefore, only a few white noise components were selected for being processed. Consequently, using the current setup, it was not possible to properly evaluate the mitigation performance provided by the harmonics method applied to the noise frequency components. However, it was expected to get similar results as in the fundamental method. In the third disturbance case, the noise would not be attenuated since the mitigation algorithm does not consider the non-static behavior of the acquired output signal. While in case with constant white noise it was predicted to record some levels of attenuation. This prediction relies on the fact that each noise frequency component would be approximated by a sinusoidal function in the time domain, even if the whole white noise signal is a non-periodic real-valued signal.

Recording the Total Harmonic Distortion (THD) of the pre and post filtered output signal in each disturbance case instead of the SNR would represent a better evaluation parameter. In this way, the mitigation performance of the harmonics method applied on the harmonic components can be compared between the three disturbance cases. As in the last two disturbance cases, the added white noise can distort the harmonic components, therefore, it can be investigated how this distortion affects the mitigation's performance.

VII. FUTURE WORK

After the simulation results, it is noticeable that the harmonics method has more potential for being used further in the development of a more complex filter suited for real-time applications. The delays recorded in the measurement, processing and injection setups represent another aspect that has to be taken into consideration when the mathematical model is derived for the harmonics method.

The passive suppression caused by real inductors and capacitors should also be analyzed further because in this simulation these components were considered ideal, where parasitic elements were not modeled. Furthermore, a better tradeoff between the physical size of these passive elements, the passive suppression rate, and the active filtering performance can be achieved by carefully adjusting the inductor and capacitor values.

Instead of searching for the harmonic components along the entire spectrum, the searching algorithm of the harmonics method can use Eq. 2 which shows the location of all harmonics. The algorithm can search in short frequency intervals centered around the harmonic locations provided by Eq. 2 therefore, the running time is expected to decrease.

The current feedback system should also be improved to facilitate the active filtering mechanism during a real-time implementation. By updating the current filtering system, a real-time simulation can be created in Simulink. One of the updates is to implement a threshold limit for the filtered signal, since complete mitigation is not possible, the algorithm should stop creating improved interference after the filtered harmonic frequency reached a certain limit value in its amplitude.

REFERENCES

[1] D. G. Holmes and T. A. Lipo, "Pulse Width Modulation for Power Converters," *Pulse Width Modul. Power Convert.*, 2003.

[2] K. Mainali and R. Oruganti, "Conducted EMI mitigation techniques for switch-mode power converters: A survey," *IEEE Trans. Power Electron.*, vol. 25, no. 9, pp. 2344–2356, 2010.

[3] F. Vasca and L. Iannelli, "Dynamics and Control of Switched Electronic Systems," *J. Chem. Inf. Model.*, vol. 53, no. 9, pp. 1689–1699, 2013.

[4] A. Bendicks *et al.*, "Wide-Frequency EMI Suppression of Stationary Clocked Systems by Injecting Successively Adapted Cancellation Signals," pp. 36–41, 2019.

[5] A. Bendicks, M. Rübartsch, and S. Frei, "Simultaneous EMI Suppression of the Input and Output Terminals of a DC / DC Converter by Injecting Multiple Synthesized Cancellation Signals," 2019, pp. 842–847.

[6] A. Bendicks, T. Dorlemann, S. Frei, N. Hees, and M. Wiegand, "Development of an Adaptive EMI Cancellation Strategy for Stationary Clocked Systems," *IEEE Int. Symp. Electromagn. Compat.*, vol. 2018-Augus, pp. 78–83, 2018.

[7] S. Soliman and M. Srinath, "Continuous and Discrete Signals and Systems," pp. 1–44, 1998.